Mon. Not. R. Astron. Soc. **000**, 000–000 (0000) Printed 18 October 2002 (MN LATEX style file v2.2)

Limits on the infrared photometric monitoring of brown dwarfs

C.A.L. Bailer-Jones* and M. Lamm
Max-Planck-Institut für Astronomie, Königstuhl 17, D-69117 Heidelberg, Germany

Submitted 7 August 2002; Accepted 17 October 2002

ABSTRACT
Recent monitoring programs of ultra cool field M and L dwarfs (low mass stars or brown dwarfs) have uncovered low amplitude photometric I-band variations which may be associated with an inhomogeneous distribution of photospheric condensates. Further evidence hints that this distribution may evolve on very short timescales, specifically of order a rotation period or less. In an attempt to study this behaviour in more detail, we have carried out a pilot program to monitor three L dwarfs in the near infrared where these objects are significantly brighter than at shorter wavelengths. We present a robust data analysis method for improving the precision and reliability of infrared photometry. No significant variability was detected in either the J or K′ bands in 2M1439 and SDSS1203 above a peak-to-peak amplitude of 0.04 mag (0.08 mag for 2M1112). The main limiting factor in achieving lower detection limits is suspected to be second order extinction effects in the Earth's atmosphere. Suggestions are given for overcoming such effects which should improve the sensitivity and reliability of infrared variability searches.

Key words: stars: low-mass, brown dwarfs – stars: variables: other – methods: data analysis – techniques: photometric – stars: individual: 2MASSW J1439284+192915 – stars: individual: SDSSp J120358.19+001550.33 – stars: individual: 2MASSW J1112257+354813

1 INTRODUCTION

Thermodynamical considerations show that dust particles form in the atmospheres of ultra cool M, L and T dwarfs (e.g. Allard et al. (2001); Burrows & Sharp (1999); Helling (2001); Lodders (1999); Lunine et al. (1989); Sharp & Huebner (1990); Tsuji et al. (1996)). This has been confirmed in many cases from the modelling of their optical and near infrared spectral energy distributions (e.g. Leggett et al. (2001); Marley et al. (2002); Schweitzer et al. (2001)(2002)). Physical models suggest that as the effective temperature drops below about 2500 K, the photosphere becomes increasingly dusty due to increased gas condensation, whereas at even lower temperatures the dust opacity is reduced due to gravitational settling of the dust below the photosphere (Ackerman & Marley (2001); Tsuji (2001)).

However, such models assume uniform horizontal distributions of this dust, whereas recent observational work has shown a significant fraction of ultra cool dwarfs to be photometrically variable at the level of 0.01–0.08 mag (Bailer-Jones & Mundt (1999)(2001); Clarke et al. (2002a)(2002b); Gelino et al. (2002); Martín et al. (2001); Nakajima et al. (2000); Tinney & Tolley (1999)). Bailer-Jones & Mundt (2001) found evidence for a rapid evolution of features on the surfaces of a few field L dwarfs. Being field objects, they are presumably part of an older population which have long lost their disks (age > 10 Myr), thus ruling out accretion hot spots or other star–disk activity as a cause of the variability. This leaves magnetic star spots or dust clouds as the most plausible candidates, although as yet there is no *direct* evidence for the physical nature of these surface features. Theoretical arguments from Gelino et al. (2002) and Subhanjoy et al. (2002) argue against the existence of spots in ultra cool dwarfs due to the low ionization fractions. On the other hand, a non-monotonic variation with spectral type in the strength of the FeH band at 9896 Å (which would be effected by iron condensation) noted by Burgasser et al. (2002) may be indicative of an inhomogeneous dust cloud coverage, at least around the L/T transition.

If the variability is due to dust, then understanding its physical, chemical and dynamical nature is central to determining the fundamental physical parameters of ultra cool dwarfs ($T_{\rm eff}$, abundances, ages etc.) and hence their formation mechanisms. Using the dusty and condensed dust models of Allard et al. (2001), one of us has recently predicted the observational signatures of different dust cloud

* Email: calj@mpia-hd.mpg.de

and spot scenarios (Bailer-Jones (2002)). This shows that there would be a distinct signature in the J and K bands for these phenomena, depending on effective temperature and feature size.

In this paper, we present the results of a pilot project to look for variability in ultra cool dwarfs through near-simultaneous J and K′ band monitoring. A comparison of the amplitudes and correlation of any variability can be compared with surface feature scenarios from various models.

2 DATA ACQUISITION AND REDUCTION

Details of the three targets monitored are given in Table 1. They were chosen from a list of sufficiently bright objects with appropriate RA/Dec for the observatory/season to represent a range of L spectral types. The targets were observed over 16 nights in March/April 2001 from the 1.23m telescope at Calar Alto, Spain, with the MAGIC camera, equipped with a 256×256 NICMOS3 array. The pixel scale was 1.15″/pix providing a field-of-view of 5′×5′. The objects were observed in both the J (50% transmission points at 1.12 and 1.40μm) and K′ (50% transmission points at 1.93 and 2.27μm) filters. Each object was monitored continuously for several hours each night (alternating between J and K′), weather conditions permitting. Table 2 shows the log of observations. The seeing varied between about 1.2″ and 2.2″ in J (poorer seeing images are not retained in the final light curves). Weather conditions varied across the run.

A problem with the NICMOS arrays is the variation of the quantum efficiency (QE) across a single pixel (intra-pixel QE variation). On account of the coarse pixel scale and undersampled photometry, this could result in a variation in the detected flux of a non-variable star as its image moves relative to the center of a pixel. For this reason, each *epoch* (point in the final light curves) is derived from 45 frames taken with a dithering macro with non-integer pixel offsets: A field is observed at each of the nine points in a 3×3 square grid, with x/y distance 12″ (10.4 pixels) between grid points. Five consecutive 5s integrations (*repeats*) are taken at each grid point, read out in double correlated readout (DCR) mode. The macro required 4.7 minutes to execute. Due to a variable bias level, the first repeat at each grid point could not be used, leaving a total of 36 usable frames. A clipped average of these points provides a single point in the final light curve (see section 3). This procedure is necessary to achieve high precision photometry with infrared arrays.

It was further found that the bias levels for repeats 2–5 were all different, although stable in time. Thus the flat fielding and sky subtraction had to be performed separately for each repeat.

Flat fields were created on each night from the differences between illuminated and non-illuminated dome flats. For each epoch, a sky image was then created from a median combination of the nine frame positions for that repeat stage (each offset to have a common flux zero point to accommodate changes in the overall background). This process removed all sources, leaving an image of the 2D background (predominantly sky brightness) variations which was subtracted from each frame.

No correction was made for nonlinearity in the flux response of the pixels. In principle, a nonlinearity can introduce apparent variability if the stars do not remain exactly in the same place on the detector or if the stars or background undergo a uniform change in brightness (e.g. due to changes in sky brightness or atmospheric extinction). However, we have calculated that such effects introduce errors in the relative photometry of much less than 1% under good conditions, and no more than 1% in the very worst case. Note that bright reference stars were avoided to reduce the influence of nonlinearity.

3 PHOTOMETRY

A reference image was established and the positions of the target and reference stars in this propagated to all other images of the field. This avoids shifting and interpolating images, which can only degrade the data quality. Photometry was carried out using the CCDCAP aperture photometry program written by K. Mighell. CCDCAP was developed to do accurate aperture photometry with small, undersampled apertures, using a bilinear pixel interpolation algorithm (see appendix B of Mighell & Rich (1995)). After detailed investigation of the magnitude error (see below) as a function of aperture size, aperture radii of 2.4 and 2.0 pixels were used for J and K′ respectively. A 'hardness' of 1.0 was used in CCDCAP, which corresponds to the maximum subdivision of a pixel. A 'drift' of 1.5 pixels in CCDCAP allowed for optimal recentering of the aperture.

Variability monitoring requires a reliable assessment of the photometric errors. Error determinations based on readout noise and Poisson statistics in the source and sky generally underestimate the true error because they ignore various systematic errors. The grid observing method outlined above is ideally suited for determining an empirical error measure based on the 36 frames taken in rapid succession. However, due to numerous bad pixels – up to four of the nine grid positions could be contaminated – simply taking the mean and standard error of these measures frequently gave poor results, because the bad pixels could bias the photometry by several magnitudes. As the PSF is undersampled, interpolation over bad pixels (and cosmic rays) was not deemed reliable (and this can only be done to make reduction convenient: it does not add information). Instead, an iterative rejection scheme was developed to remove bad photometry. First the median and its standard deviation, σ, were determined from all 36 measures. If σ exceeded a threshold, the highest 8 and lowest 8 measures were rejected, typically corresponding to all measures at four grid positions. The median is then re-established. Iterative clipping of points more than n-σ about the median was then done to remove outliers (each iteration starting with all 36 measures so that re-inclusion was possible). The initial threshold stage is required because the median of 36 points containing just a few bad measures can result in an unrepresentative median and hence large amounts of data being clipped. A threshold of 0.2 mag and n=5 were used, although the results are not sensitive to these values. The iterative clipping converged after 0–3 iterations. This procedure was found to be very robust, both excluding obvious bad pixels but resulting in more than 32 (of 36) measures being retained in the majority of cases.

The mean of the remaining N measurements was taken

Table 1. Targets observed. The reference is the discovery paper and provides the spectral type and IAU name. The photometry is from 2MASS from the archive compiled by Kirkpatrick (2003).

name	IAU name	SpT	J	K_s	reference
2M1439	2MASSW J1439284+192915	L1	12.76	11.58	Reid et al. (2000)
SDSS1203	SDSSp J120358.19+001550.33	L3	14.02	12.48	Fan et al. (2000)
2M1112	2MASSW J1112257+354813	L4.5	14.57	12.69	Kirkpatrick et al. (2000)

Table 2. Log of number of observations retained in final light curve for each object. AJD is defined as JD−2450000.

Night	AJD	2M1112		SDSS1203		2M1439		weather
		J	K′	J	K′	J	K′	
2	1990.5	24	27					some cloud
3	1991.5	8	10					cloudy
4	1992.5	12	13			41	41	mostly clear
5	1993.5	11	12			21	21	clear
6	1994.5					32	32	some cloud, later clear
7	1995.5	3	3			42	42	some cloud, later clear
8	1996.5							rain (no observations)
9	1997.5					6	6	high humidity and cloud
10	1998.5			7	7	26	26	mostly clear
11	1999.5							fog (no observations)
12	2000.5							fog (no observations)
13	2001.5			39	39	10	10	clear
14	2002.5			42	42	10	10	clear
15	2003.5	43	44			6	6	clear
16	2004.5					15	15	clear, high humidity
17	2005.5			16	16	23	23	mostly clear
Total		101	109	104	104	232	232	

to be the final magnitude for that epoch. As these are all independent measurements of the same thing,[1] the appropriate error, δm, in this measure is the standard error in this mean, i.e. $\sigma/\sqrt{N}$. We found that the theoretical errors produced by IRAF's apphot task (based on source Poisson noise and detector read-out noise) – using the same aperture sizes – were as much as ten times smaller, i.e. grossly underestimated. This demonstrates the importance of using empirical error measures in infrared photometry, at least with NICMOS3 arrays.

Photometry was obtained in this manner for the target and reference stars in all frames. Differential photometry was performed as described in Bailer-Jones & Mundt (2001) to produce a light curve for the target relative to the average flux of the reference stars. This removes first order (wavelength independent) variations in the sky extinction between epochs.[2] Light curves were similarly constructed for each reference star relative to all the other reference stars. 6, 8 and 5 reference stars were retained for 2M1112, SDSS1203 and 2M1439 respectively.

In what follows, *light curve* shall always mean the relative magnitude light curve, i.e. the magnitude of the star relative to its particular set of reference stars. By *reference level* we mean the time series of the reference magitude for the L dwarf target, i.e. the magnitude formed from the average of the fluxes of the target's reference stars (see Bailer-Jones & Mundt (2001) section 3.3).

4 LIGHT CURVE ANALYSIS

The light curves for the target star and reference stars were plotted and examined visually for features. The χ^2 test as used by Bailer-Jones & Mundt (2001) was also applied to look for variability across the whole data set and within individual nights. When interpreted as probabilities of variability on the assumption of Gaussian errors, these χ^2 values often indicated significant variability ($p << 0.01$) in both the target and some of the reference stars. Assuming that not all of these really are intrinsically variable at this level, this implies one or more of the following: 1. the photometric errors have been underestimated; 2. the errors are non-Gaussian; 3. the *relative* photometry is not representative of the *intrinsic* brightness of the stars. Point (1) seems unlikely given the thorough testing of the method described in section 3 to evaluate the errors. Point (2) is generally true due to outliers: this will inflate all χ^2 values for all stars, meaning that one should adopt a conservative threshold for flagging variability (i.e. a small value of the probability, p, or equivalently a higher χ^2 value). However, this would not be magnitude dependent so would not lead to a differential ef-

[1] This assumes that the star does not vary over 4.7 minutes. If it does, then this error is an overestimate of the true error.

[2] This is true provided the extinction is constant across the 5′ image field size averaged across the $70\cos\delta$ arcmins on the sky through which the field moves during the 4.7 min macro execution time.

fect between the target and reference stars. Thus the relative values of χ^2 can still be used as an indication of variability. Point (3) could be problematic on account of colour effects in the extinction variation, as will be discussed in section 6.

As we have near-simultaneous observations in two bands, J and K′, we introduce a parameter to look for correlated changes in the relative magnitudes. For a given star at epoch number t, this parameter is defined as

$$Q(t) = \sum_{t'=1}^{t'=t} \frac{m_{\rm J}(t') - m_{\rm J}(t'-1)}{\delta m_{\rm J}} \cdot \frac{m_{\rm K'}(t') - m_{\rm K'}(t'-1)}{\delta m_{\rm K'}}$$

where $m_{\rm J}(t')$ is the relative J magnitude of the star at epoch t' and similarly for $m_{\rm K'}(t')$. $\delta m_{\rm J}$ is the error in $m_{\rm J}(t') - m_{\rm J}(t'-1)$, obtained from the quadrature sum of the empirical error measures, δm, for each epoch (see section 3). Each of the two terms on the right hand side of this equation gives the change in relative magnitude from one epoch to the next in the units of the random error; significant changes have a modulus larger than unity. As the two terms, one for J and one for K′, are multiplied together, correlated changes in the two bands give a positive contribution to the sum; anticorrelated changes a negative contribution. Thus if the star shows a series of correlated changes, Q will become more positive; if they are anticorrelated it becomes more negative. If changes are random, i.e. sometimes correlated and sometimes anticorrelated, Q will do a random walk; in particular it has an expectation value of zero and variance of t (the number of epochs). By comparing the variation in Q for the target with that for its reference stars, we can see whether the target tends to show a greater level of colour correlated (or colour anticorrelated) changes than the reference stars. This is summarized by $Q_{\rm s}$, the difference between the maximum and minimum values of Q across all epochs.

As cool spots and dust features effect the radiative flux over a wide wavelength range in the optical and infrared, the evolution of such features will produce *some* kind of correlated or anticorrelated change in the J and K′ bands and hence some pattern in the Q parameter. This is the motivation for the Q parameter. The specific relative amplitudes in these bands depends on the physical mechanism (spots or clouds or something else) and of course on the specific atmospheric models used. For example, making predictions based on the models by Allard et al. (2001), we see that dust variations in early L dwarfs produce anticorrelated J/K′ variations, whereas star spots produce correlated ones (Bailer-Jones (2002)). Different relative amplitudes may be predicted when making different assumptions in the models, e.g. with a different dust grain size distribution or treatment of convection.

Our J and K′ observations are not strictly simultaneous. However, for SDSS1203 and 2M1439, a strict pairing of K′ observations immediately after J observations was maintained in the final light curves, and Q has been evaluated using this pairing. For various reasons this was not possible with 2M1112, so Q values have not been calculated for this field. A summary of the relative photometry, errors and $Q_{\rm s}$ is given in Table 3.

Table 3. Photometry of targets and their reference stars. $\rm J_r$ and $\rm K'_r$ are the magnitudes of the reference stars and $\rm (J\text{-}K')_r$ their colours, relative to the target (and averaged across all epochs). $\overline{\delta m_d}$ is the average across epochs of the relative magnitude errors, as given by equation 4 in Bailer-Jones & Mundt (2001). $Q_{\rm s}$ is defined in the text.

	$\rm J_r$	$\overline{\delta m_d}$	$\rm K'_r$	$\overline{\delta m_d}$	$\rm (J\text{-}K')_r$	$Q_{\rm s}$
SDSS1203	0.000	0.016	0.000	0.012	0.000	9
ref. 1	-1.620	0.010	-0.849	0.013	-0.771	7
ref. 2	0.578	0.012	0.448	0.014	-1.026	15
ref. 3	0.829	0.021	1.757	0.035	-0.928	11
ref. 4	0.640	0.019	1.614	0.030	-0.974	7
ref. 5	0.932	0.026	1.701	0.033	-0.769	9
ref. 6	1.467	0.037	2.562	0.067	-1.095	7
ref. 7	1.242	0.035	1.516	0.032	-0.274	6
ref. 8	1.433	0.033	2.376	0.053	-0.943	10
2M1439	0.000	0.016	0.000	0.018	0.000	15
ref. 1	-0.559	0.017	0.101	0.023	-0.660	8
ref. 2	0.707	0.018	1.431	0.024	-0.724	23
ref. 3	1.953	0.026	2.699	0.042	-0.746	8
ref. 4	2.257	0.034	3.102	0.058	-0.845	12
ref. 5	2.557	0.038	2.901	0.050	-0.344	15

5 RESULTS

SDSS1203 Calculated across the entire data set, SDSS1203 gives χ^2 values of 200 and 306 for J and K′ respectively. These formally correspond to very small p values (a test with 103 degrees of freedom) but, as noted in section 4, we may expect χ^2 to be large due to outliers across this large number of observations. Indeed, the reference stars also give large χ^2 values: ranging from 114 to 158 (for J) and 98 to 155 (for K′). Ignoring the formal p values and just looking at the relative χ^2 values, we see that SDSS1203 is indeed more variable than any of the reference stars in both filters.

Fig. 1 shows the J and K′ light curves across the four nights of observation. There are several points which deviate from the mean by more than 3σ, although generally the variability is quite weak (< 0.05 mag deviation). On night 13, there is a dip in K′ at around AJD 2001.4. A similar but opposite effect is seen in reference star 2 (although not ref. 1) and the egress from this dip is accompanied by a rise in the reference level, so this is probably a telluric effect. The 4σ jump in J at AJD 2001.51 is not accompanied by any similar feature in the reference stars or reference level so could be intrinsic to SDSS1203, although it is neither large nor that statistically significant. The J dip at AJD 2002.63, on the other hand, *is* accompanied by a dip in the reference level (but not the reference stars). This could be due to a colour dependent variation in the extinction (see section 6). We also note that SDSS1203 appeared to be brighter in K′ at the beginning of night 17, an effect which is marginally significant and cannot obviously be reduced to the behaviour of the reference stars or reference level.

The Q parameter in Fig. 1 shows no long lasting colour correlated variations. Moreover, the range of Q, given by $Q_{\rm s}$, is no larger than for the reference stars (Table 3). The J/K′ correlation coefficient, ρ, is slightly larger for SDSS1203 than the other stars (ρ=0.34 against ρ=0.07–0.24 for the reference stars), although it is still small.

We conclude that there is no good evidence for variabil-

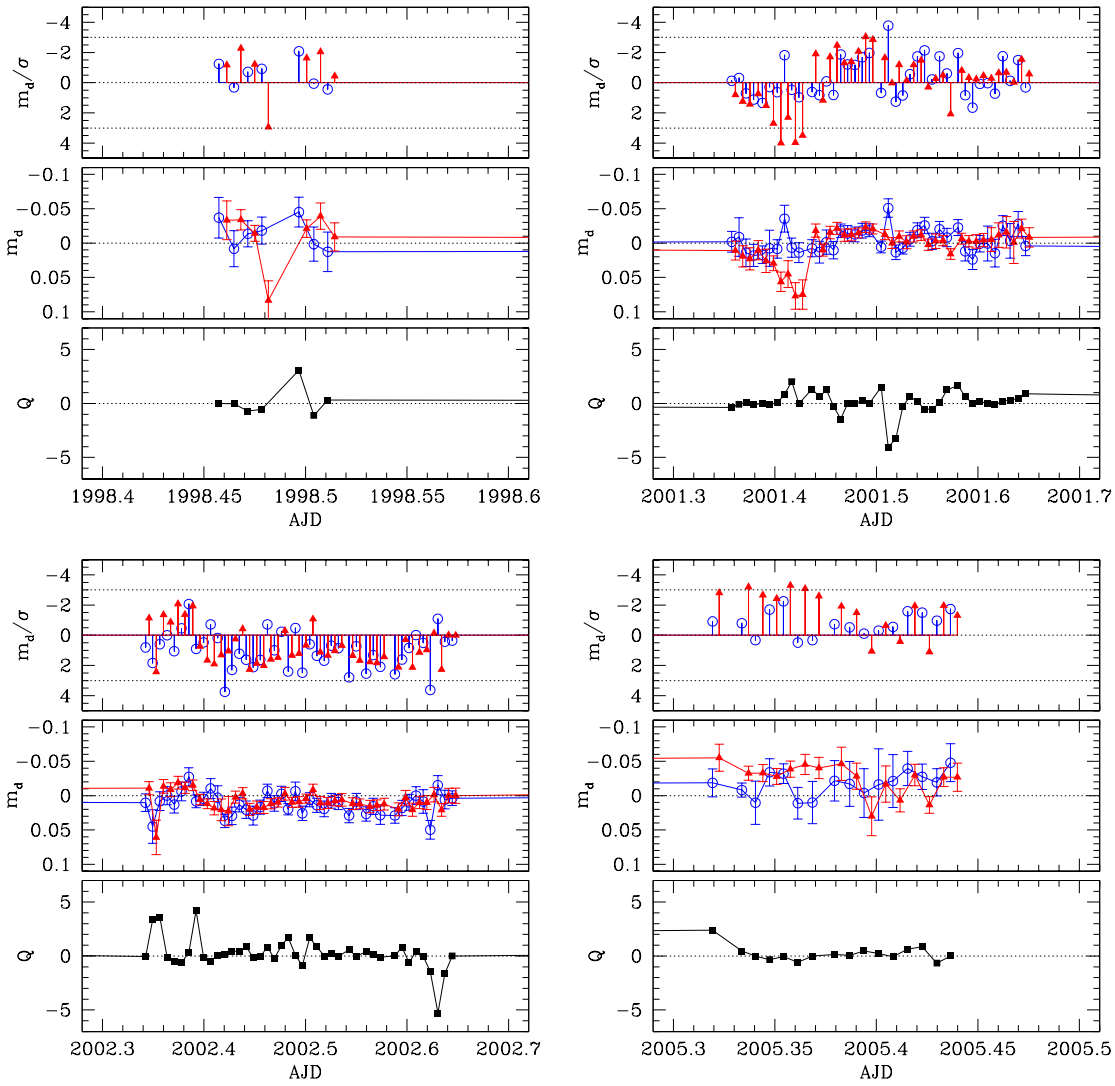

Figure 1. Light curves for SDSS1203, one plot for each night (nights 10, 13, 14 and 17). The open circles (blue) are for the J band and the closed triangles (red) for the K′ band. The middle panel for each night shows the relative light curve of SDSS1203 (with a common magnitude zero point for all nights equal to the average relative magnitude across all epochs). The top panel for each night shows this light curve in units of the photometric errors at each epoch, which can be used to judge the significance of any deviations. The bottom panel plots the $Q(t)$ value, defined by the equation in section 4.

ity in SDSS1203 from these data. SDSS1203 was found to be variable in the I-band by Bailer-Jones & Mundt (2001), primarily due to an apparent brightening of the object over a duration of one to two hours. As far as we could tell, those data were taken under good observing conditions near culmination of the object (i.e. very small airmass changes) so we do not believe that result was an artifact due to the Earth's atmosphere.

2M1439 As with SDSS1203, this object shows more significant variability than any of the reference stars for both J and K′ according to the χ^2 test applied to all data. However, its Q values, as well as the correlations between J and K′ and J and J−K′ are no larger than for some of the reference stars.

It can be seen in Fig. 2 that the K′ light curve of 2M1439 dims by 0.14 mag over a period of five hours from AJD 1992.4 on night 4. Although no such trend (or opposite trend) is seen in the light curve of the reference stars individually, the opposite trend is seen in the reference level with a scale of 0.4 magnitudes, indicating that all of the reference stars increased in brightness (Fig. 3). This coincides with the field rising – from an airmass of 2.6 to 1.05 – so is presumably just due to the usual decrease in extinction with decreasing airmass. However, while the reference stars brighten by 0.4 mag, 2M1439 brightens by only 0.26 mag. This is possible if the extinction coefficient has a strong gradient across the K′ band and if 2M1439 has a different flux gradient from the reference stars. In this case, second order (colour) effects in the terrestrial extinction may become

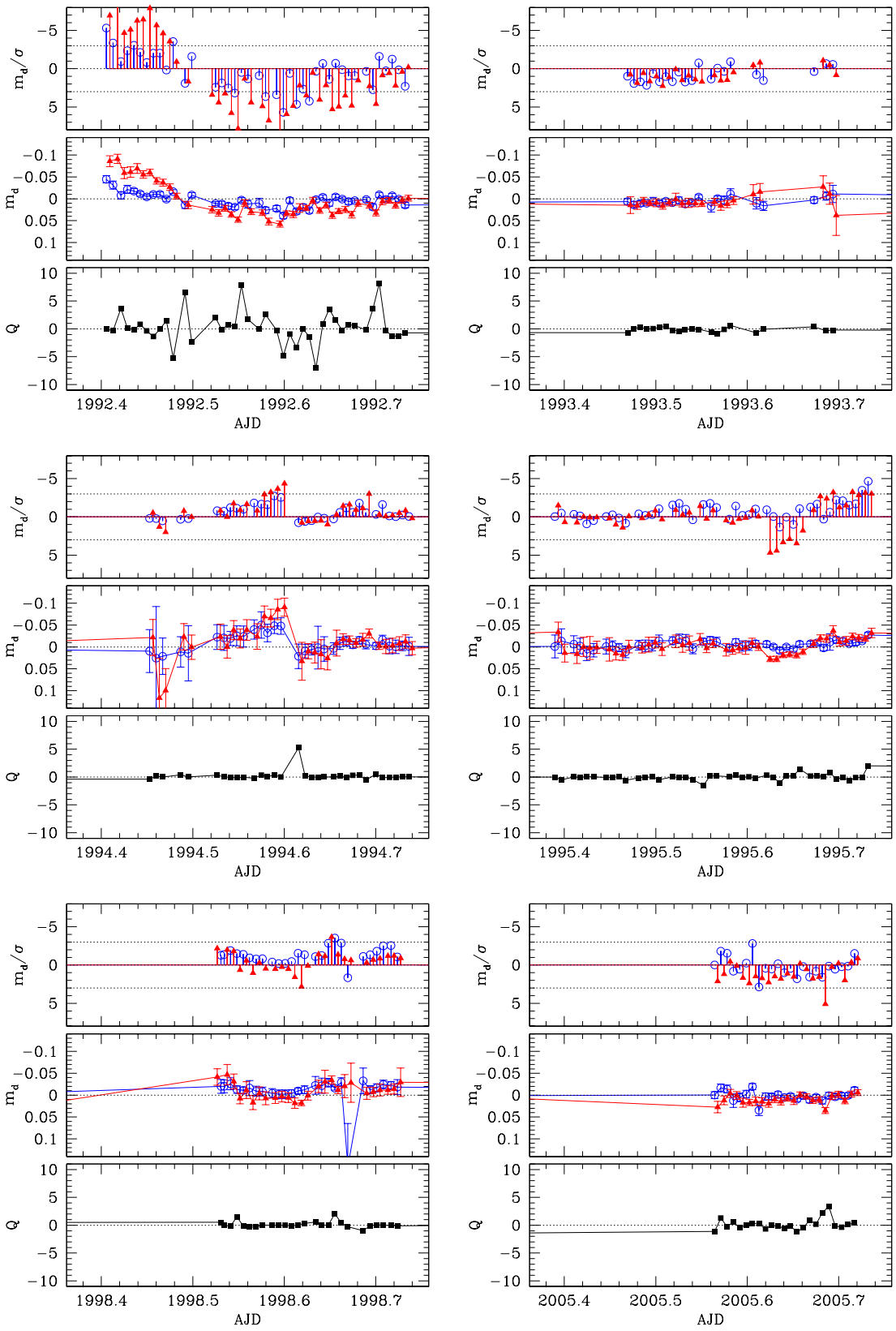

Figure 2. Light curves for 2M1439 (see caption to Fig. 1 for an explanation). Light curves are shown only for 6 of the 11 nights on which data were taken (see Table 2), specifically for nights 4, 5, 6, 7, 10 and 12.

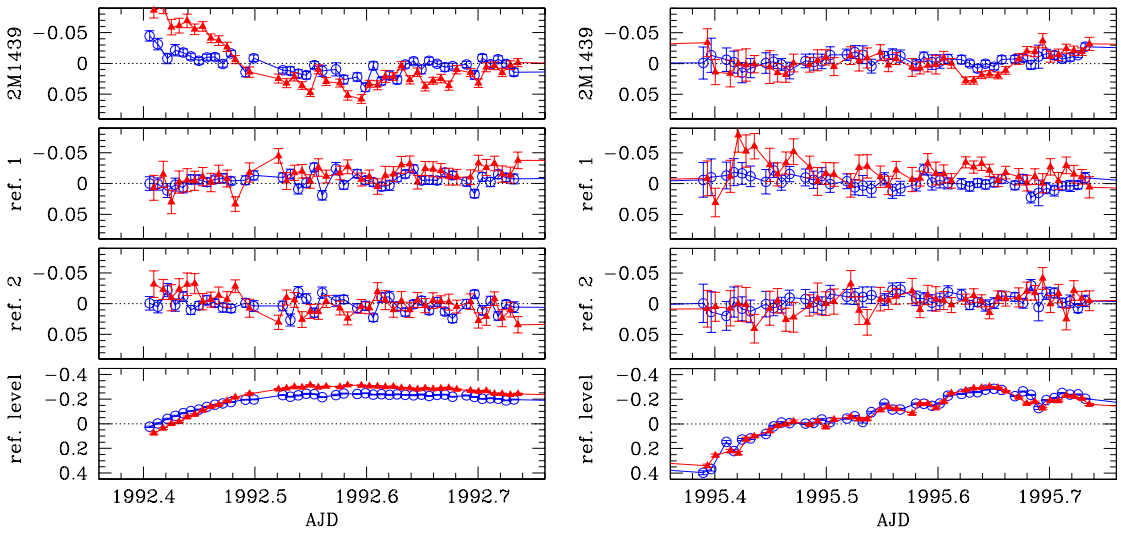

Figure 3. Relative magnitude light curves for 2M1439 (top row), the first (i.e. brightest) reference star (second row) and the second (i.e. next brightest) reference star (third row). The bottom row shows the variation in the reference level for 2M1439. The reference level is the magnitude formed from the average of the fluxes of all five reference stars shown in Table 3 (with the average of this level over all epochs subtracted). As in the other figures, the open circles (blue) are for the J band and the closed triangles (red) for the K′ band. The left panel is for night 4, the right panel for night 7.

important (see section 6). The same effect is seen in the J band (reference level brightens by 0.35 mag, 2M1439 dims relative to this by 0.07 mag).

However, on night 7 we see the same brightening of the reference level due to decreasing airmass (0.65 mag in both bands from airmass 2.8 to 1.05) but without any trend or significant variability in the light curves of either the reference stars or 2M1439 (see right hand panel in Fig. 3). Clearly, different atmospheric conditions must have prevailed on this night than on night 4.

Correlated changes of up to 1 magnitude in J and K′ are found in the reference level at the beginning of night 6, caused by thin clouds and humidity. Correlated changes with amplitude up to 0.1 mag are also seen in the light curves of the reference stars and 2M1439, indicating that these large extinction variations have not cancelled out in the relative photometry. This is presumably caused by water vapour changes associated with the clouds (see section 6).

In conclusion, most of the features which account for the higher variability in 2M1439 (compared to the reference stars) appear to be related to terrestrial atmospheric phenomena.

2M1439 has previously been monitored in the I-band by Bailer-Jones & Mundt (2001) and by Gelino et al. (2002). Neither found good evidence for variability above about 0.01 mag, the former from temporally-dense observations (48 observations spread over four nights) and the latter over longer timescales (a few observations per night over 40 nights).

2M1112 This light curve shows some variations which at first sight would be of significance, but on closer inspection appear to be due to variations in the reference level. These are not qualitatively different from the "problematic" variations seen in the other two targets, discussed above.

We performed a frequency-domain search for periodic variations using two methods, the CLEAN and Lomb-Scargle periodograms. These methods yielded consistent results and showed no evidence for periodic variations in SDSS1203 or 2M1439. As implemented, these methods are known to be effective at detecting even low signal-to-noise periodic signals (Lamm et al. (2003)).

6 SECOND ORDER EXTINCTION EFFECTS

The method of relative photometry employed in this program (and all those referred to in section 1) makes the implicit assumption that the Earth's atmospheric extinction is the same for the target star as for the reference stars. However, the extinction coefficient varies with wavelength, so if the target and reference stars have different spectral energy distributions (SEDs), their wavelength integrated extinctions are also different. This is relevant when monitoring ultra cool dwarfs, as the reference stars will usually be significantly hotter and hence bluer in the optical and near infrared (see Table 3). This would not matter for relative photometry if the extinction did not vary in time or space. But extinction does vary polychromatically with airmass and atmospheric conditions, thus introducing a change in the relative magnitude between stars with different SEDs. Such effects are referred to as second order extinction.

In the visible, the extinction is dominated by molecular (Rayleigh) and aerosol scattering and generally shows a smooth decrease with increasing wavelength. In this case, colour effects are either small or a broad band colour term can be used to correct relative photometry (also as a function of airmass). In the near infrared, however, the extinction is dominated by molecular absorption, particularly of

H_2O, CO_2 and O_3, which show much sharper variations with wavelength. Precipitable water vapour and ozone concentrations in particular can vary rapidly in time and space. *Thus even under apparently good observing conditions, second order extinction effects can have a significant impact on high precision, differential, broad band infrared photometry.* Note that terrestial water clouds and fog are dominated by large ($>>1\,\mu$m) water droplets, so these cause a scattering of visible and infrared light with only a weak wavelength dependence ($\lambda^{-\alpha}$, where $0 < \alpha < 1$). Nonetheless, some absorption also occurs in the liquid drops themselves which does show rapid changes in some wavelength ranges, although in the optical at least the colour dependence of terrestrial cloud extinction appears to be small (Honeycutt (1971); Serkowski (1970)). However, where there are clouds there is presumably also a high water *vapour* column density, with the result that clouds would contribute to second order extinction.

Unfortuntately, we cannot quantify the effects of second order extinction on our data, because we have no independent measure of the atmospheric constituents – in particular the column density of the precipitable water vapour – and we would further require an appropriate atmospheric model matched to the Calar Alto conditions at the time. Moreover we do not know the SEDs of the reference stars: the broad band J–K′ colour is too undersampled to determine the integrated extinction from a water spectrum (Young (1989)).

An idea of the scale of the problem can be found from reference to the models of J and K extinction at Kitt Peak for a cool giant (T_{eff}=4000 K) and Vega (T_{eff}=9650 K) from Manduca & Bell (1979). At low water column density, the differential extinction between the two stars ($E_{4000}-E_{9650}$) is 0.049 mag at J and 0.002 mag at K. Increasing the water column density by a factor of 35 changes these to 0.067 mag at J and 0.001 mag at K. Thus increasing the precipitable water density increases the differential extinction (so decreases the apparent brightness of a cool star relative to a hotter star) by approximately 0.02 mag at J and −0.001 mag at K.[3] The actual precipitable water column density experienced during our observations could be larger, so it is not implausible that water vapour changes cause the apparent variability we see in the L dwarfs. Contrary to the figures given above, however, we generally see similar amplitude variations in J as in K′. But our K′ filter extends further into the blueward telluric absorption band than does the Johnson K band of Manduca & Bell and these figures are quite sensitive to the band profile. Also, our target (and probably reference) stars have much lower temperatures than 4000 K and 9650 K.

Changes in airmass under stable conditions can also change the relative photometry. For example, Manduca & Bell show that the J band magnitude of a cool giant relative to Vega would be at least 0.01 mag higher when measured at airmass 2.0 than at airmass 1.0. The effect is much smaller in the K band, however, so this may not be cause of the dimming of 2M1439 on night 4 discussed in section 5 (see Fig. 3), as there the dimming is larger in K′ than J. However, this may again be due to the differences between the K and K′ bands and the SEDs of the stars. Recall that no such dimming was seen on night 7 for the same airmass change, perhaps indicating different causes of extinction on these nights.

The fact that both SDSS1203 and 2M1439 showed larger χ^2 values for J and K′ than the reference stars can be attributed to the likelihood that the reference stars have more similar SEDs to each other than to L dwarfs, so that differential extinction effects between any one reference star and all the other reference stars (which form its reference level) are much smaller. Hence the reference stars show less variability.

Second order extinction is less of a problem in the optical ($\lambda < 0.65\,\mu$m), but here most brown dwarfs are far too faint to be monitored. The I band (~ 0.78–$0.92\,\mu$m) is a good compromise. This too is intersected by a water absorption band centered at $0.81\,\mu$m, but this band is much weaker than those effecting the J and K bands (e.g. McCord & Clark (1979)).

7 CONCLUSIONS

The prime requirements of any search for variability are (1) a measurement of the scale of the variability *intrinsic* to the source, and (2) an accurate determination of the observational errors in these measurements. However the analysis is done, a variability detection relies on the former being significantly larger than the latter.

We have developed an observation and data reduction technique which gives an accurate and reliable determination of the photometric errors, arising from the source, background, detector and effect of the data processing (see section 3).

One of the main problems with ground-based monitoring is variations in the extinction (scattering plus absorption) of the Earth's atmosphere. The standard procedure of differential photometry was used to give a measure of intrinsic variability. Using this, some evidence for variability was found in the observed L dwarfs. However, closer analysis has shown that this measure is probably "contaminated" by second order extinction effects in the Earth's atmosphere (see section 6). Although we have no direct evidence for this, it seems the most plausible cause of the observed variability given the features we have described and the elimination of other potential causes. We therefore conclude that we have no good evidence for intrinsic variability in any of the three L dwarfs monitored. None of these objects showed significant correlations in their J and K′ light curves, as evidenced by correlation plots and our Q parameter. Some such (anti)correlation would be expected if the variability is caused by cool spots or dust features. Upper limits on the peak-to-peak amplitude of *persistent* variability are set by the scatter in the light curves under the most stable Earth atmospheric conditions. For both J and K′, these limits are set at 0.04 mag for SDSS1203 and 2M1439 and 0.08 for 2M1112.

As late M, L and T dwarfs are at their brightest in the near infrared (0.9–2.5 μm) and show spectral signatures which could discriminate between various surface feature scenarios (Bailer-Jones (2002)), this is a desirable wavelength range for variability monitoring. We have shown that high *precision* differential photometry (random errors of less

[3] Derived from Tables IIa and IIb of Manduca & Bell for Johnson filters at an airmass of 1.5.

than two percent) can be achieved on L dwarfs with infrared arrays. However, as a measure of the intrinsic variability in L dwarfs, broad band differential infrared photometry appears to be limited in *accuracy* to a few percent by variations in terrestrial molecular extinction, in particular precipitable water vapour. These second order extinction effects could be reduced in one or more ways:

(i) use of passbands which avoid molecular extinction, in particular use of better designed (narrower) J and K′ filters to avoid the strong H_2O bands which generally intersect these "standard" filters[4];

(ii) use of narrower band filters, which reduces the effect of second order extinction[5] (this would obviously require a larger telescope or longer integration times; the latter will be unacceptable for detecting short-term variability);

(iii) use of specially designed filters to monitor the dominant molecular absorption (in particular H_2O) from which the broad band relative photometry could, in principle, be corrected (Angione (1987)). This could be done using a multi-channel camera. However, additional spectroscopic observations are required to calibrate the measures and so apply the correction. Nonetheless, some kind of time-dependent monitoring of extinction would at least allow one to recognise when observing conditions were variable;

(iv) observing from very dry sites under atmospherically stable conditions. Space-based observations remove all problems related to second order extinction. A strong discriminant between candidate surface features in brown dwarfs is the variability signatures in the water absorption bands at 1.35–1.45μm and 1.80–2.00μm (e.g. Bailer-Jones (2002). These bands cannot be reliably monitored from the ground, providing another argument for space-based observations.

ACKNOWLEDGEMENTS

We are grateful to Ken Mighell for use of his CCDCAP algorithm and for useful information on its application and interpretation.

REFERENCES

Ackerman A.S., Marley M.S., 2001, ApJ 556, 872
Allard F., Hauschildt P.H., Alexander D.R., Tamanai A., Schweitzer A., 2001, ApJ 556, 357
Angione R.J., 1987, PASP 99, 895
Angione R.J., 1989, in *Infrared extinction and standardization*, Lecture Notes in Physics 341, E.F. Milone (ed.), Springer-Verlag, Berlin, p. 25
Bailer-Jones C.A.L., 2002, A&A 389, 963
Bailer-Jones C.A.L., Mundt R., 1999, A&A 348, 800
Bailer-Jones C.A.L., Mundt R., 2001, A&A 367, 218, Erratum: A&A, 374, 1071
Burgasser A.J., Marley M.S., Ackerman A.S., Saumon D., Lodders K., Dahn C.C., Harris H.C., Kirkpatrick J.D., 2002b, ApJ 571, L151
Burrows A., Sharp C.M., 1999, ApJ 512, 843
Clarke F.J., Tinney C.G., Covey K.R., 2002a, MNRAS 332, 361
Clarke F.J., Oppenheimer B.R., Tinney C.G., 2002b, MNRAS, in press
Fan X., Knapp G.R., Strauss M.R., et al., 2000, AJ 119, 928
Gelino C.R., Marley M.S., Holtzman J.A., Ackerman A.S., Lodders K., 2002, ApJ, in press
Helling C., Oevermann M., Lüttke M.J.H., Klein R., Sedlmayr E., 2001, A&A 376, 194
Honeycutt R.K., 1971, PASP 83, 502
Kirkpatrick J.D., Reid I.N., Liebert J., et al., 2000, AJ 120, 447
Kirkpatrick J.D., 2003, in ASP Conf. Ser. vol. 211, in press
`http://spider.ipac.caltech.edu/staff/davy/ARCHIVE/`
Lamm M., Bailer-Jones C.A.L., Mundt R., Herbst W., 2003, in preparation
Leggett S.K., Allard F., Geballe T.R., Hauschildt P.H., Schweitzer A., 2001, ApJ, 548, 508–518
Lodders K., 1999, ApJ 519, 793
Lunine J.I., Hubbard W.B., Burrows A., Wang Y-P., Garlow K., 1989, ApJ 338, 314
Manduca A., Bell R.A., 1979, PASP 91, 848
Marley M.S., Seager S., Saumon D., Lodders K., Ackerman A.S., Freedman R., Fan X., 2002, ApJ 568, 335
Martín E.L., Zapatero Osorio M.R., Lehto H.J., 2001, ApJ, 557, 822
McCord T.B., Clark R.N., 1979, PASP 91, 571
Mighell K.J., Rich R.M., 1995, AJ 110, 1649
Nakajima T., Tsuji T., Maihara T., et al., 2000, PASJ 52, 87
Reid I.N., Kirkpatrick J.D., Gizis J.E., et al., 2000, AJ 119, 369
Schweitzer A., Gizis J.E., Hauschildt P.H., Allard F., Reid I.N., 2001, ApJ 555, 368
Schweitzer A., Gizis J.E., Hauschildt P.H., Allard F., Howard E.M., Kirkpatrick J.D., 2002, ApJ 566, 435
Serkowski K., 1970, PASP 82, 908
Sharp C.M., Huebner W.F., 1990, ApJSS 72, 417
Subhanjoy M., Basri G., Shu F., Allard F., Chabrier G., 2002, ApJ 571, 469
Tinney C.G., Tolley A.J., 1999, MNRAS 304, 119
Tsuji T., Ohnaka K., Aoki W., 1996, A&A 305, L1
Tsuji T., 2001, in *Ultracool dwarfs: New Spectral Types L and T*, H.R.A. Jones & Steele I. (eds.), Springer-Verlag, Heidelberg, pp. 9–25
Young A.T., 1989, in *Infrared extinction and standardization*, Lecture Notes in Physics 341, E.F. Milone (ed.), Springer-Verlag, Berlin, p. 6

[4] There is significant variance between the profiles of filters called I, Z, J, H and K at different observatories, so there is no such thing as a "standard" infrared filter set, although most Z, J and K filters are intersected by significant water absorption bands.

[5] A variation on this method has been used by Bailer-Jones (2002), in which an L dwarf was monitored spectrophotometrically relative to another star in the spectrograph slit. The relative photometry was then performed independently in each narrow wavelength bin (0.002 μm), reducing effects of second order extinction to well below other error sources.